Proceedings of ASME Turbo Expo 2025
Turbomachinery Technical Conference and Exposition
GT2025
June 16–20, 2025, Memphis, Tennessee, USA

GT2025-153625

INTEGRATING TURBINE BLADE COOLING WITH EXHAUST GAS RECIRCULATION FOR ENHANCED CARBON CAPTURE IN COMBINED CYCLE GAS TURBINE

Abhishek Dubey
Thermochemical Power Group (TPG)
University of Genova,
16145 Genova, Italy
abhishek.dubey@edu.unige.it

Antoine Verhaeghe
University of Mons (UMONS)
Rue de l'Epargne, 56
7000 Mons, Belgium
antoine.verhaeghe@umons.ac.be

Ward De Paepe
University of Mons (UMONS)
Rue de l'Epargne, 56
7000 Mons, Belgium
ward.depaepe@umons.ac.be

Alessandro Sorce
Thermochemical Power Group (TPG)
University of Genova,
16145 Genova, Italy
alessandro.sorce@unige.it

ABSTRACT

In this paper, we present the investigation towards the feasibility of turbine blade cooling using Exhaust Gas from the Exhaust Gas Recirculation (EGR) in Combined Cycle Gas Turbine (CCGT) power plants for enhanced carbon capture (CC). The study has been performed due to the need to develop more economical solutions for carbon capture in current CCGTs during the transition towards net zero. Commercially mature CCGTs are the most efficient technology for power generation through fossil fuels and are widely used due to their higher flexibility, reliability and lower emissions compared to other power generation technologies. Post-combustion CC offers a solution to reduce CO_2 emissions from CCGTs. However, the low CO_2 concentration in exhaust gas results in a high CC energy demand, leading to high operating costs (OPEX), and the large volumetric exhaust flow rate requires large CC equipment and, thus, high capital costs (CAPEX). Based on theoretical studies, it is generally accepted that EGR should be applied in current CCGTs to reduce exhaust flow and increase its exhaust CO_2 concentration. However, as EGR reduces oxygen concentration at the combustor inlet, the allowable recirculation of exhaust gas is limited by the minimum oxygen content required in the combustor to avoid flame instability and carbon monoxide emission. In this study, we explore an innovative approach that uses exhaust gas for cooling the turbine blade, referred to as exhaust gas cooling (EGC), as a potential solution for further increasing the CO_2 concentration in the exhaust and reducing exhaust mass flow without impact on combustion, leading to smaller CC units and lower CC energy consumption in existing utility-scale CCGTs, which are currently cooled using compressor bleed air. An H-class Mitsubishi M701JAC power plant with three pressure level reheat bottoming cycle is modelled in WTEMP (Web-based Thermo-Economic Modular Program) software, a modular cycle analysis tool developed at the University of Genova. Carbon capture from the exhaust gas is performed using a Monoethanolamine (MEA) CC unit, modelled in Aspen Plus V14. A fraction of recirculated exhaust gas, compressed by an auxiliary EGC compressor, is used for cooling the turbine blades and the remaining is mixed with inlet air before gas turbine intake. Simulations were performed while maintaining an oxygen concentration of 16% (by mol.) at the combustor inlet. The impact of EGR-based turbine cooling on CCGT full load performance is evaluated in terms of efficiency and CC plant penalty. Results showed that, compared to conventional EGR, for the same O_2 fraction at the combustor inlet, replacing compressor bleed air with exhaust gas for turbine cooling can increase the EGR ratio from 0.35 to 0.40 and reduce the exhaust mass flow by 91.2 kg/s (14.4%) in an H-class CCGT, leading to an increase in CO_2 exhaust concentration by 15.32%. As a result, the size of the CC columns and their heat consumption were slightly reduced. With EGC, the power plant efficiency also increased by around 2%, mainly due to the use of exhaust gas with high specific heat for cooling. Therefore, the study demonstrates a novel concept that can be implemented in current CCGT power plants for enhanced carbon capture.

Keywords: gas turbine, combined cycle power plants, carbon capture, exhaust gas recirculation, turbine cooling, exhaust gas cooling, efficiency

NOMENCLATURE

Symbols

Bi_{met}	biot number of turbine blade metal
Bi_{TBC}	biot number of thermal barrier coating
c_p	specific heat capacity [$Jkg^{-1}K^{-1}$]
ε_o	cooling effectiveness
ε_f	film cooling effectiveness
K_{cool}	cooling flow factor
m	mass flow rate [kgs^{-1}]
η	efficiency [%]
η_{int}	internal convective cooling efficiency
Q	heat [J]
P	pressure [Pa]
R	gas constant [$Jkg^{-1}K^{-1}$]
T	temperature [K]
γ	ratio of specific heats
ε_f	film cooling effectiveness
Ψ	cooling flow ratio
X	molar concentration
Subscripts	
a	air
adwall	adiabatic wall temperature
bl	turbine blade
c	compression
cl	cooling fluid
ca	air cooling medium
cex	exhaust cooling medium
in	inlet
g	main gas flow in turbine
out	outlet
tot	total
Acronyms	
3PRH	three pressure level with reheat
CCGT	combined cycle gas turbine
COP	coefficient of performance
CC	carbon capture
CPR	compressor pressure ratio
DCC	direct contact cooler
EGC	exhaust gas cooling
EGR	exhaust gas recirculation
GT	gas turbine
HRSG	heat recovery steam generator
IP	intermediate pressure level
LP	low-pressure level
LHV	lower heating value of fuel [Jkg^{-1}]
OEM	original equipment manufacturer
TIT	turbine inlet temperature [K]
TOT	turbine outlet temperature [K]

1. INTRODUCTION

Due to increasing global efforts towards decarbonization, more than 560 GW of new renewable capacity was added in 2023 [1]. Investments in clean energy projects are approaching USD 2 trillion each year [1], and renewable power generation capacity is expected to increase from 4,250 GW today to around 10,000 GW in 2030 [1]. Despite the increasing renewable penetration, global CO_2 emissions from electricity generation increased by 1% in 2023 [2]. Fortunately, the share of fossil fuel in global electricity generation is expected to decline from 61% in 2023 to 54% in 2026 [2], and electricity-related CO_2 emissions are expected to decline at an unprecedented average rate of 4% between 2023 and 2026 [2]. This projection can reduce the global CO_2 intensity from the current level of 455 g_{CO2}/kWh to 400 g_{CO2}/kWh in 2026. The global electricity demand is also parallelly rising. Compared to 2022, it increased by 2.2% in 2023 and is expected to rise at a faster annual rate of 3.4% in the next three years [2]. Also, because more than 60% of electricity is still produced from fossil fuels, the demand for natural gas is, thus, projected to increase annually by 2.5% over the next decade [1,3]. Therefore, although CO_2 emissions are projected to reduce in coming years due to renewable penetration, the rate of reduction is still too slow. Even with strict policies and regulations, conventional power plants are projected to produce 74% of the electricity in 2040 [4] and therefore, more innovative solutions are required for faster reduction of carbon emissions from the power sector.

At present, combined cycle gas turbines (CCGTs) are the most efficient way of producing electricity. For instance, the latest 9HA.02 H-Class CCGT from General Electric has an electrical efficiency of 64.1% [5]. CCGTs produce lower CO_2 emissions than traditional coal-fired plants, have a low load capability of up to 20% [6] and a fast ramp rate of up to 88 MW/minute [5]. Modern heavy-duty CCGT power plants have an average CO_2 intensity of 345 g_{CO2}/kWh at full load and 417 g_{CO2}/kWh at minimum environmental compliant load [6]. The corresponding values for a large subcritical coal plant are 775 g_{CO2}/kWh at full load and 866 g_{CO2}/kWh at minimum compliant load [6]. CCGTs are widely used to stabilize power demand and address grid fluctuations, with increasing renewable penetration [7–9]. Therefore, CCGT power plants are going to play a crucial role in meeting the rising demand during the transition phase in the short and mid-term. The gas turbine market for power is forecasted to grow at a compound annual growth rate (CAGR) of 5.1% from 2022 to 2030 [10]. To reach net zero by 2050, global temperature rise should be limited to 1.5 °C, and therefore, several innovative technologies such as hydrogen combustion, alternative hydrocarbon fuels and more efficient power plant technologies are being developed. Most modern CCGTs offer 50% hydrogen capability and efforts are ongoing towards the possibility of 100% hydrogen combustion [5]. However, these technologies are either still in the research phase or only practical for short-scale deployment. Hence, most currently operational CCGT plants still operate with natural gas and release substantial amounts of CO_2. As the power sector and the global economy are strongly dependent on these CCGTs, it is not possible to shut them down completely. Therefore, to achieve net-zero emissions, the only option is to develop technologies to reduce the carbon footprint of these existing plants, which will be operating for several decades.

Consequently, carbon capture (CC) and storage have emerged as an important technology to reduce CO_2 emissions in current power plants. [11,12]. Carbon capture in modern systems can achieve up to 95% CO_2 reduction or even higher with optimized solutions [13], thereby capturing emissions that would otherwise enter the atmosphere and contribute to global warming. Post-combustion carbon capture based on chemical absorption is an attractive solution for CO_2 sequestration in current natural gas-fired CCGT power plants. Conventional chemical absorption through Monoethanolamine (MEA) or Methyldiethanolamine (MDEA) is a mature and effective technology [14], but it requires high thermal energy for solvent regeneration, i.e. the reboiler energy, which reduces plant efficiency [14,15]. Furthermore, CCGT power plants have a lower CO_2 concentration of 3-4.5% (mol.) in exhaust [13] compared to coal-fired plants in which CO_2 concentration is 12-14% (mol.). This low concentration, coupled with high flow rates, requires large CC equipment, resulting in high CAPEX and OPEX of CC units in current natural gas-fired CCGTs [16]. Reboiler energy can be supplied in a bolt-on solution where the reboiler steam is supplied through a separate external boiler or in a steam-integrated solution where thermal energy is supplied by steam extraction from the CCGT steam turbine. Gibbins et al. [17] studied the technical and economic feasibility of a range of CC solutions for natural gas and coal plants, including bolt-on and steam integration solutions. In an 800 MW_e CCGT plant, the bolt-on solution reduced efficiency by 13 p.p. and power by 6.6%. On the other hand, the steam integration solution reduced efficiency by 7 p.p. and power by 13% [17].

As per several theoretical studies, implementing exhaust gas recirculation (EGR), where a part of exhaust gas from the stack is recirculated and mixed with the gas turbine inlet air [18], can increase CO_2 concentration in the exhaust while simultaneously reducing exhaust mass flow. As shown by Li et al. [15], a 50% EGR ratio can increase the molar CO_2 concentration in exhaust from 3.8% to 7.9% while simultaneously reducing exhaust gas mass flow by 51% and reboiler energy consumption by 8.1%, providing efficiency increment of 0.4% compared to without EGR case [15]. These reductions in exhaust flow and CC energy demand also decrease the CC efficiency penalty and the CC plant size, which translates into lower capital expenditure [18]. For instance, an EGR ratio of 50% could reduce the CAPEX of an amine plant by 21.1% [19].

Implementing EGR has some technical challenges as well. Firstly, the maximum amount of recirculated exhaust gas or EGR ratio is limited by the minimum O_2 concentration required at the combustor inlet. A high EGR ratio can reduce the O_2 concentration low enough to disrupt stable combustion operation or might lead to flameout [20]. Moreover, low O_2 concentration can also increase CO emissions by reducing peak flame temperature, thereby preventing oxidation of CO. For instance, in an experimental study by Ditaranto et al. [21], it was found that combustion could be sustained at an O_2 concentration of 14 vol% but with excessively high CO and unburned hydrocarbon emission, indicating that an EGR ratio higher than 35% could be difficult to achieve in practice. Similarly, ElKady et al. [20] also experimentally demonstrated that the GE F-class heavy-duty DLN combustor could handle EGR ratios up to 0.35 without major modifications and highlighted increased CO emission with EGR as a limiting factor. For current combustors, the minimum required O_2 concentration is in the range of 14-16% O_2 (mol.).

Secondly, EGR also impacts turbomachinery performance slightly by altering the fluid properties at the compressor inlet. Because exhaust gas is at slightly higher temperatures than ambient air, the inlet temperature is increased, and density is reduced with EGR, reducing the mass/volume flow. Although exhaust gases are cooled before mixing with gas turbine inlet air, it is not possible to cool them down below ambient air temperature without using additional equipment for refrigeration purposes. As mentioned by Li et al. [15], a 50% EGR reduces volumetric flow by 1.61 % and mass flow by 1.04 %. Since the impact is small, high EGR can be practically handled without any modifications by existing turbomachinery. Despite these technicalities, EGR in CCGT plants continues to be an attractive approach for more efficient carbon capture in CCGTs. As an example, GE Vernova has launched a new project in 2024 to build the world's first gas-fired power station with carbon capture and storage by implementing EGR in GE's 9HA.02 gas turbine. The plant will be constructed as a part of the Net Zero Teesside (NZT) power project in the United Kingdom. It is being developed to capture up to 2 million tons of CO_2 per year and its start-up is expected in 2028 [22].

Biliyok et al. [23] studied the benefit of EGR in a 440 MW_e natural gas-fired CCGT. On implementing CO_2 capture without EGR, CCGT net power was found to reduce by 14.7%. However, employing 40% EGR showed a recovery of 10 MW_e net power due to the reduced CC penalty from increased CO_2 concentration in exhaust [23]. Botero et al. [18] investigated EGT in a 400 MW_e CCGT plan to find the best integration strategy through an integrated amine reboiler with the optimization of steam integration. The best obtained solution showed an efficiency reduction of 8 p.p. (percentage points) and a power reduction of 12%. Sammak et al. [13] studied the bolt-on and steam-integrated solutions at different EGR ratios and EGR return temperatures and found that the steam-integrated solution can decrease additional CC CAPEX expenditure by 30% compared to the bolt-on solution.

Along with steam integration techniques in CCGT with EGR, alternate and more efficient amine-based solvents based on their lower heat of regeneration and higher CO_2 loading capacity are also being investigated to increase the CO_2 capture rate with less reboiler energy [24–26]. More recently, Verhaeghe et al. [25] studied the impact of steam integration strategies on CCGT plant performance with two different solvents, namely MEA and a blend of MDEA and piperazine (PZ). Results showed that extracting steam from IP/LP crossover and using MDEA/PZ blend instead of MEA can increase the CCGT plant efficiency by 0.5 p.p. Apart from alternate solvents, research works are also underway to develop less energy extensive solvent regeneration methods and processes [26]. For instance, Baudoux [27] et al. recently studied various configurations of solvent regeneration in a 770 MW CCGT to achieve a more economical CC process. Lean vapour recompression combined with rich solvent preheating using reboiler condensate was found to be the most efficient configuration, and it reduced the equivalent energy consumption of the conventional CC plant by 7.3%, increasing the CCGT net electrical efficiency by 0.5% [27].

The studies related to the economic benefits of EGR are limited in the literature however, some estimates are available. For instance, Sammak et al. [13] studied carbon capture in a 636 MW CCGT and showed that without EGR, the absorption system itself contributed to 44.3% of total CC plant CAPEX among the four main segments of CC plant (DCC, absorption system, stripper system, and CO_2 compression train). In fact, the absorption system and DCC together contributed 60% of the total CC equipment cost. Such a high share of absorption and DCC in CAPEX is because the size of these systems is governed by the volumetric flow rate, which is quite high for utility-scale CCGT power plants. In the same study, Sammak et al. [13] reported that a 30 % EGR could reduce the total CAPEX of the CC plant by

37%. In a nutshell, carbon capture in CCGT puts significant performance and economic penalties on the net power and efficiency of the plant due to the high flow rate and low CO_2 concentration in exhaust. It affects the plant economics significantly, and therefore more innovative solutions are required to reduce CC penalty in order to ensure economic viability and widespread implementation of CC in CCGT.

The present study investigates the viability of a novel concept of integrating EGR with turbine blade cooling, hereafter referred to as Exhaust Gas Cooling (EGC), for enhanced carbon capture in currently natural gas-fired CCGTs. Using exhaust gas for turbine cooling instead of conventional compressor bleed air has two potential advantages. Firstly, it uses all the fresh air where it is needed (i.e. to maintain the O_2 concentration at the combustor inlet), substituting where the presence of oxygen is not required. So, the EGC provides an additional enrichment of exhaust gas with CO_2 with a benefit on the CC side. Secondly, the higher specific heat of exhaust gases used for blade cooling can reduce cooling flow and provide thermodynamic benefits on the cycle. In fact, increased CO_2 concentration through EGC can theoretically reduce the energy needed for solvent regeneration and reduce the CC penalty on plant performance. To the best of the author's knowledge, the current work is the first attempt to study the integration of exhaust gas with turbine cooling for CO_2 enrichment in CCGT exhaust flow.

This paper is structured as follows: first, the methodology is described mainly, focusing on the CCGT model and the turbine cooling model in the WTEMP software. Then, the carbon capture model in Aspen Plus V14 is described. After that, results are analyzed in terms of increased CO_2 concentration in the exhaust and the impact of EGC on CCGT performance, followed by the conclusions.

2. METHODOLOGY

2.1. CCGT Model and Validation

This study is focused towards carbon capture in existing CCGT power plants. Therefore, a CCGT with a gas turbine cycle consisting of four turbine stages connected to a 3PRH bottoming cycle was modelled in the WTEMP software. Each turbine stage consisted of one stator row and one rotor row. Six out of eight turbine rows (first three stages) were cooled. This CCGT model was then validated with the nominal design point specifications of the latest H-Class 50 Hz industrial CCGT from major original equipment manufacturers (OEMs). WTEMP (Web-based Thermo-Economic Modular Program) software is developed by Thermochemical Power Group (TPG) at the University of Genova. It is a modular and flexible tool for thermo-economic analysis and optimization of innovative energy systems. It is used here because of its upgradability and extensive implementation in the past for the gas turbine cycles [31,33,34].

Performance specifications for Ansaldo GT36-S5 and Mitsubishi M701JAC were acquired from the Turbomachinery International handbook 2024 [35], while that for General Electric (GE) 9HA.02 was obtained from the OEM website [5]. In general, rating specifications disclosed by OEMs are limited to CPR, exhaust mass flow and TOT, efficiency (LHV basis) and power output for simple cycle and combined cycle plants. All OEM ratings are provided at ISO baseload conditions (15°C, 1 atm and 60% relative humidity) and 100% methane fuel with fuel preheating and 3PRH HRSG configuration [35,36]. However, several important parameters required for modelling these CCGTs, such as TIT, cooling flows, BC pressure levels, condenser pressure, heat losses and auxiliary losses, are not disclosed as they are propriety information of OEMs. Therefore, for theoretical validation of these plants, one is forced to make reasonable assumptions for unknown parameters. For validating these plant models in WTEMP, all available input parameters from OEM, such as inlet conditions and compressor pressure ratio were maintained the same as reported by OEM. The values of other unavailable cycle parameters were calibrated to minimize the difference in performance parameters (electrical efficiency and power) between the WTEMP model and practical CCGT. The values of the calibrated parameters were kept within the reasonable practical range based on information available in the literature. All calibrated parameters were kept the same for three CCGTs, and their values are listed in Table 1 and Table 2 for the GT cycle and bottoming cycle, respectively. This is the typical approach for validating complex CCGT models with real power plants [36–38], and a more detailed description of such an approach and associated challenges can be found in the work done by Chiesa et al. [37] and Gülen [36].

TABLE 1: PARAMETERS IN GT CYCLE MODEL.

Parameter	Value
Inlet Air Temperature (°C)	15
Inlet Air Pressure (bar)	1.013
Relative Humidity (%)	60
Compressor polytropic efficiency (%)	90
Turbine polytropic efficiency (%)	90
Combustion efficiency (%)	99.9
Combustor pressure drop (%)	5
Mechanical Efficiency (%)	99.5
Blade metal temperature (°C)	890
Generator Efficiency (%)	98.85

In validation of the CCGT model, all the compressor bleed air for turbine cooling was extracted from the final compressor row at discharge temperature, and fuel was preheated in an external heat exchanger from the intermediate pressure drum.

TABLE 2: PARAMETERS IN BOTTOMING CYCLE MODEL.

Parameter	Value
LP Pressure (bar)	5
IP Pressure (bar)	45
HP Pressure (bar)	160
Economizer sub-cool (°C)	8
Evaporator pinch-point ΔT(°C)	10
Superheater approach ΔT(°C)	15
HP Steam Turbine Efficiency (%)	90
IP Steam Turbine Efficiency (%)	91
LP Steam Turbine Efficiency (%)	91
Water Side Pressure Drop (%)	1.5
Heat loss SH, EV & EC (%)	0.25
Pump Adiabatic Efficiency (%)	85
Electrical Engine Efficiency (%)	97

TABLE 3: RESULTS OF CCGT MODEL VALIDATION IN WTEMP. NUMBERS INSIDE THE BRACKET ARE PERCENTAGE ERRORS BETWEEN WTEMP MODEL AND SPECIFICATIONS BY OEM.

	GT36-S5 (Ansaldo Energia)		**M701JAC** (Mitsubishi)		**9HA.02** (General Electric)	
Parameter	**OEM** [35]	**WTEMP**	**OEM** [35]	**WTEMP**	**OEM** [5]	**WTEMP**
Simple cycle power (MW_e)	538.0	541.1 (0.58)	574.0	570.9 (-0.55)	571.0	571.4 (0.06)
Simple cycle efficiency (%)	42.8	43.79 (2.32)	43.4	43.42 (0.04)	44.0	43.1 (-2.07)
Pressure ratio	26.0	26.0	25.0	25.0	23.8	23.8
TOT (°C)	621.0	612.1 (-1.43)	646.0	647.9 (0.29)	640.0	647.4 (1.16)
TIT (°C)	-	1570	-	1640	-	1610
Exhaust mass flow (kg/s)	1020	1020	1024	1024	1040	1040
Combined cycle power (MW_e)	760.0	762.3 (0.30)	840.0	825.3 (-1.74)	838.0	829.1 (-1.03)
Combined cycle efficiency (%)	62.6	62.6 (-0.03)	64.0	63.7 (-0.53)	64.1	63.4 (-1.06)
Gas Turbine Power (MW_e)	533.0	528.6 (-0.83)	570.9	557.1 (-2.42)	561.0	559.0 (-0.36)
Steam Turbine Power (MW_e)	227.0	233.7 (2.94)	269.1	268.2 (-0.32)	277.0	270.1 (-2.49)
Non-chargeable cooling flow (%)	-	8.6	-	10.2	-	9.3
Chargeable cooling flow (%)	-	5.9	-	6.3	-	5.9

- Non-chargeable cooling flow is the cooling flow for the first stator and all other cooling flows are chargeable. Values are given as a percentage of compressor inlet air.

TIT was defined as the temperature at the combustor outlet or first stator inlet in this work. TIT was then calibrated through heat balance in WTEMP to minimize the error in performance specifications. As a result of continuous efforts to increase TIT, most modern H-Class CCGTs have TIT of 1600°C or higher. Mitsubishi has already commercialized CCGT with 1650°C TIT in 2020 [39] and has a development program towards 1700°C TIT [40]. Similarly, the HA class of plants from GE are advertised with 1600°C TIT technology. Apart from TIT, TOT is another important parameter in CCGTs. Practical HRSGs are typically fed with TOT in the range of 550-650°C [36], and the latest industrial CCGTs can even have TOT higher than 650°C [35]. Therefore, a maximum live steam temperature of 640°C was used for M701JAC and 9HA.02 and 620°C were used for GT36-S5 in the validation. Also, a condenser pressure of 0.04 bar was assumed for M701JAC and 9HA.02 and 0.06 bar was assumed for GT36-S5. Due to the unavailability of these data for the current year from OEM, reasonable values had to be taken based on literature and OEM data from previous years. The final results of the validation process are shown in Table 3. All the error values between OEM and WTEMP data are less than 3%. Mitsubishi M701JAC power plant was then selected as the technology for implementation of EGR based turbine cooling, due to its highest amount of cooling flow. Only the validation was performed with 100% methane, and thereafter all subsequent simulations were performed with natural gas, with the following molar composition: CH_4:0.9071; C_2H_6:0.0603; C_3H_8:0.0099; C_4H_{10}:0.003; N_2:0.0112; CO_2:0.0085. The lower heating value of the natural gas was 47.7 MJ/kg.

After the validation, the carbon capture plant was integrated with three different CCGT configurations in this work: i) conventional CCGT without EGR, ii) CCGT with EGR and conventional turbine cooling and iii) CCGT with EGR where a part of the recirculated exhaust gas is used to cool the three turbine stages (instead of air from compressor) and the remaining recirculated gas is fed into the gas turbine inlet.

2.2. Turbine Cooling Model

In this work, each turbine stage consisted of a stator and a rotor. The expansion process of a cooled turbine stage is shown in Fig. 1. In the first step, the stator cooling air is mixed with the main gas flow, and the resulting mixture is expanded in the rotor. A mixing pressure loss equal to 0.07Ψ was considered for the mixing of the main gas flow and cooling flow in the stator based on the correlation developed by Horlock et al. [28]. The cooling air for the rotor is mixed after the expansion, and the resulting mixture enters the subsequent stage. This model of turbine expansion with stator and rotor cooling is widely implemented in literature and effectively able to capture practical trends [29,30].

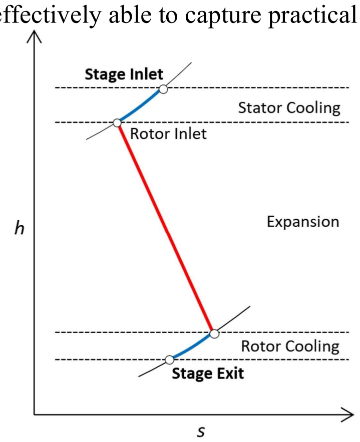

FIGURE 1: EXPANSION MODEL OF A COOLED TURBINE STAGE [31].

The cooling flow was estimated based on the approach developed by Wilcock et al. [32]. It allows the prediction of cooling flow ratio (Ψ) based on different cooling technology levels (CTL) expressed in terms of five parameters (Eqs. 1-5), namely cooling flow factor (K_{cool}), internal convective cooling efficiency (η_{int}), film cooling effectiveness (ε_f), Biot number of turbine blade metal (Bi_{met}) and Biot number of thermal barrier coating (Bi_{TBC}). For a given main gas temperature (T_g), allowable blade metal temperature (T_{bl}) and cooling flow inlet temperature

($T_{ca,in}$), the cooling effectiveness (ε_o) is calculated by Eq. 1, and then Ψ is calculated from Eq. 5 using the parameters listed in Table 4 for the blade cooling model used in this work.

$$\varepsilon_o = \frac{(T_g - T_{bl})}{(T_g - T_{ca,in})} \tag{1}$$

$$\eta_{int} = \left(\frac{T_{ca,out} - T_{ca,in}}{T_{bl} - T_{ca,in}}\right) \tag{2}$$

$$\varepsilon_f = \left(\frac{T_g - T_{adwall}}{T_g - T_{ca,out}}\right) \tag{3}$$

$$Bi = Bi_{TBC} - Bi_{met}\left(\frac{\varepsilon_o - \varepsilon_f}{1 - \varepsilon_o}\right) \tag{4}$$

$$\Psi = \frac{m_{ca}}{m_g} = \frac{K_{cool}}{(1+Bi)}\left(\frac{\varepsilon_o - \varepsilon_f\,[1 - \eta_{int}(1 - \varepsilon_o)]}{\eta_{int}(1 - \varepsilon_o)}\right) \tag{5}$$

In real turbines, K_{cool} is a function of complex flow and blade geometry parameters such as surface area, mean heat transfer coefficient and Stanton. For convenience, Wilcock et al. [32] considered a constant value of K_{cool}, which was calibrated with real engine data.

Moreover, to account for the non-uniformity of temperature at the combustor outlet, the main gas temperature at the first stator inlet was modified as per Eq. 6 for calculating Ψ [32].

$$T_{g,max} = T_g + K_{comb}\,\Delta T_{comb} \tag{6}$$

where $T_{g,max}$ is the maximum temperature at the inlet of the first stator, K_{comb} is the pattern factor and ΔT_{comb} is the combustor temperature rise. The value K_{comb} was 0.15, the same as the one used by Wilcock [32].

TABLE 4: PARAMETERS OF BLADE COOLING MODEL USED IN THIS WORK.

Parameter	Symbol	Value
Cooling flow factor	K_{cool}	0.045
Internal convective cooling efficiency	η_{int}	0.70
Film cooling effectiveness	ε_f	0.40
Biot number of blade metal	Bi_{met}	0.15
Biot number of thermal barrier coating	Bi_{TBC}	0.30

It is important to mention that this model used technology-level parameters for predicting cooling flow, with compressor bleed air as the cooling medium without information about cooling medium properties or blade geometry. Since the cooling technology parameters were tuned to real engine data, the effect of heat exchange properties of air as the cooling medium was accounted for within the model. In order to use this model for exhaust gas that has higher specific heat, the cooling flow ratio with exhaust gas was calculated by keeping the heat transfer from blade to the cooling medium the same as with air. With the cooling flow rate for air known, $T_{ca,out}$ which is temperature of cooling air exiting the blade, was obtained from Eq. 2. Next, Q_{bl}, total heat transferred from blade to cooling air, was calculated from heat balance in turbine blade system as per Eq. 7.

$$Q_{bl} = m_{ca}(c_{p,ca,out}T_{ca,out} - c_{p,ca,in}T_{ca,in}) \tag{7}$$

where m_{ca} is the mass flow of cooling air, $c_{p,ca,out}$ and $c_{p,ca,in}$ are the specific heats for cooling air at the outlet and inlet of the blade, respectively. After that, m_{cex}, exhaust cooling flow required to transfer Q_{bl} amount of heat was calculated from Eq. 8. The temperature of cooling fluid at blade exit ($T_{cex,out}$) was the same as that of air, as defined by the value of internal cooling efficiency, η_{int}, in Eq. 2.

$$Q_{bl} = m_{cex}(c_{p,cex,out}T_{cex,out} - c_{p,cex,in}T_{cex,in}) \tag{8}$$

This approach of same blade heat transfer for different cooling mediums allowed capturing the effect of higher c_p of exhaust gas in terms of reduced cooling flow (shown in Fig. 2 for TIT of 1500°C).

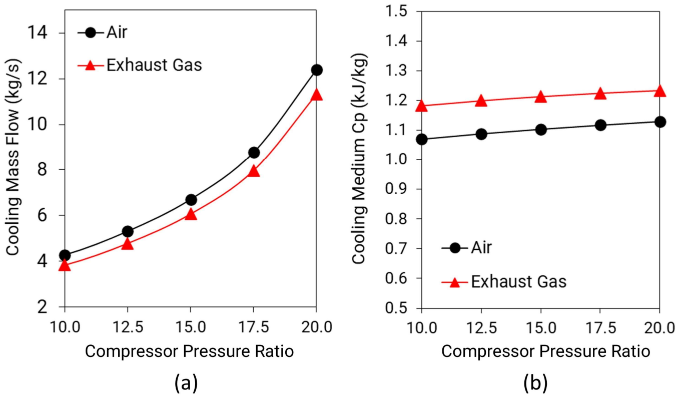

FIGURE 2: REPLACING AIR WITH EXHAUST GAS FOR COOLING REDUCES THE COOLING FLOW (a) DUE TO HIGHER SPECIFIC HEAT OF EXHAUST GASES (b).

2.3. Exhaust Gas Recirculation Implementation

The layout of the M701JAC CCGT with EGC (exhaust gas cooling for turbine blades) is shown in Figure 3. Note that the same gas turbine cycle with 3PRH bottoming cycle layout (parts shown in black in Fig. 3) was used as CCGT layout for validation. The only difference was that the three turbine stages were cooled from the compressor bleed air, and there was no EGR or CC plant. An EGR loop was then included in the CCGT model to recirculate part of the exhaust gas (stream 2) into the gas turbine. For the EGC case, an auxiliary EGC compressor was added to compress the ambient pressure exhaust gas (stream 5) to the required pressure for entry in each turbine row. The EGR loop was modelled using Aspen Plus V14 [41]. The EGR loop consists of a direct contact cooler (DCC) to cool down the exhaust gas and remove the condensed water. A splitter was used to separate the cooled gas (stream 3) for recirculating a part of it (stream 4) into the gas turbine and sending the remaining gas (stream 6) to the carbon capture unit. Two different blowers were used to push these split gas streams. A mixer was used to mix the exhaust gas with ambient air before entering the compressor (stream 1). The DCC was modelled with a RadFrac unit and composed of IMPT packings. The diameter of the DCC for each case was determined to avoid flooding and the height was set to 10m for all the cases. A design specification was used to set the gas approach to liquid temperature to 5°C by adjusting the cooling water flow rate. The temperature of the cooling water at the inlet of the DCC was set to 25°C after passing through an air cooler. The amount of recirculated gas, defined by the EGR ratio, was selected as the maximum value that would maintain an O_2 content of 16 mol.% at the inlet of the combustion chamber in the gas turbine for

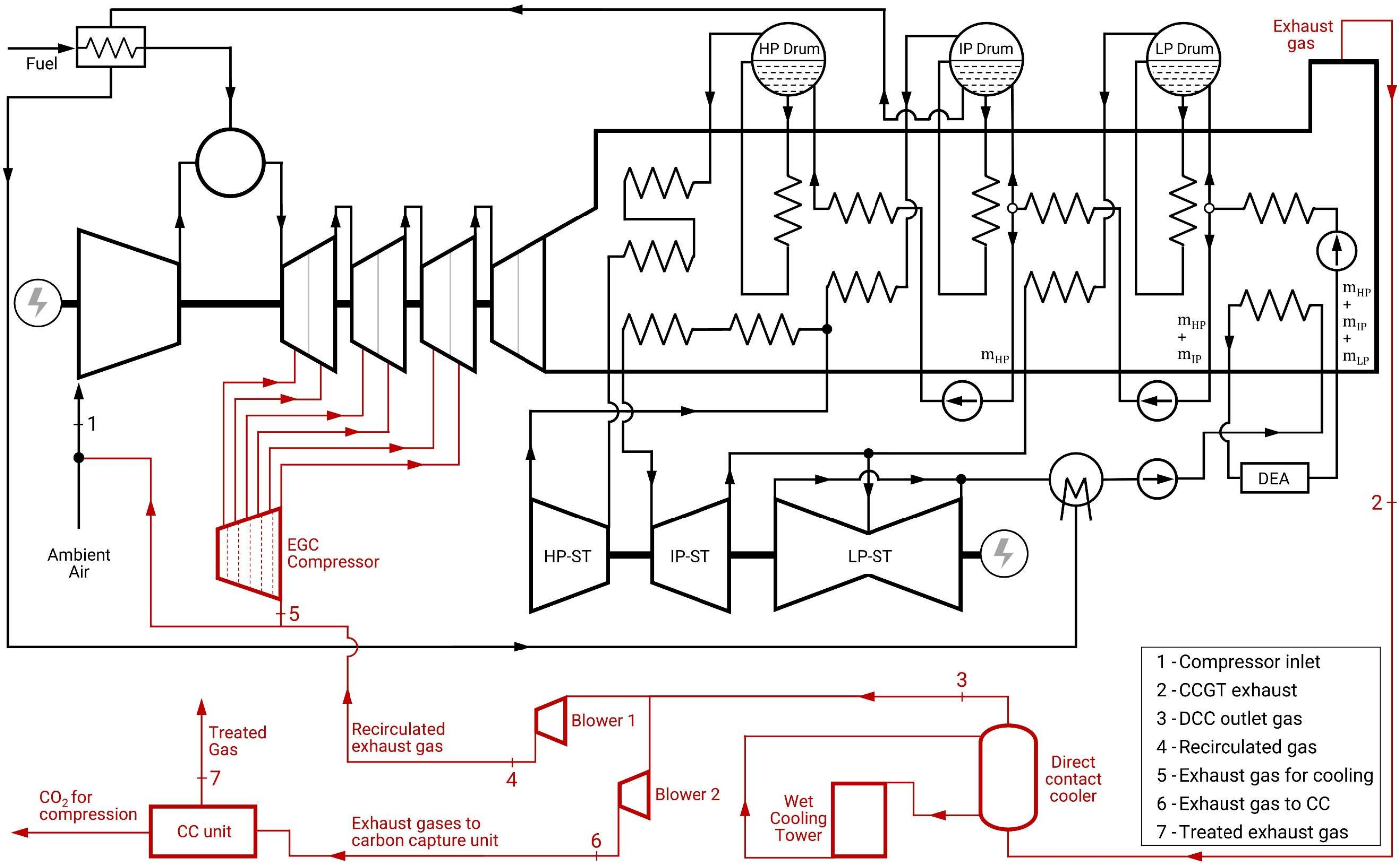

FIGURE 3: SCHEMATIC DIAGRAM OF THE COMBINED CYCLE CONSISTING OF A GAS TURBINE WITH FOUR STAGES (THREE COOLED STAGES) CONNECTED TO THREE PRESSURE LEVEL REHEAT (3PRH) BOTTOMING CYCLE.

combustion stability [21,25]. Therefore, for both conventional EGR and EGC, a different EGR ratio was set. The isentropic efficiency of the blower was set at 80%, and the outlet pressures were set to 1.013 bar to push the gas towards the compressor inlet. A slightly higher pressure of 1.1 bar was set for another blower for pushing exhaust gas towards the CC to overcome pressure losses in the absorber column.

2.4. Carbon Capture Model and Integration

The conventional amine(s)-based absorption-regeneration process, shown in Fig. 4, was used in this study. The benchmark 30 wt.% Monoethanolamine (MEA) aqueous solution was used as the solvent. The CC process consisted of two packed columns: an absorber and a stripper. The cooled exhaust gas was fed to the bottom of the absorber (8), while the liquid solvent is introduced at the top. In the absorber (1), the liquid solvent absorbs the CO_2 from the gas phase by chemical reactions, resulting in a CO_2 enriched solvent (rich solvent) exiting from the bottom. The exhaust gas was released at the top of the absorber in the atmosphere with a lower CO_2 content, depending on the capture rate. The absorption process typically occurs at 40°C and under atmospheric pressure. After the absorption process, the rich solvent is pumped (2) through a heat exchanger (3), where it undergoes heating by the hot solvent, leaving the stripper before being introduced at the top of the column. The solvent is regenerated in the stripper (4) by heat input through the bottom

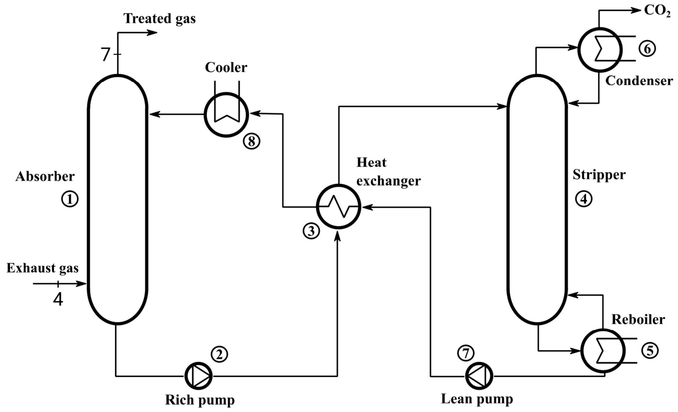

FIGURE 4: THE CC PLANT BASED ON CONVENTIONAL MEA-BASED ABSORPTION-REGENERATION PROCESS.

reboiler (5). The regeneration process takes place within a temperature range of 100-120°C and a pressure range of 1.2-2 bar for the MEA solvent. The CO_2 stripped from the solvent exits the top of the stripper and passes through a condenser (6) to remove most of the water. Then, the produced CO_2 is typically compressed and injected into the CO_2 transport network. The regenerated solvent, leaving the bottom of the stripper, is pumped (7) into the internal heat exchanger (3) and then cooled (8) before being reintroduced in the absorber. A water-washed process is usually installed at the top of both columns to extract solvent residues from the exhaust gas or CO_2 stream.

The CC plant was modelled using Aspen Plus V14 [41]. The CC model has been developed and validated in previous works [25,42]. The thermodynamic models used are the Electrolyte Non-Random Two Liquid (ENRTL) model for electrolyte properties [43] in a liquid phase and the PC-SAFT equation of state for the vapour phase. The model parameters are taken from [44]. Specific kinetic parameters are described in [45]. Both the absorber and the stripper columns are modelled with RadFrac units using the rate-based approach. As the packing used is IMTP#40 in both columns, the Hanley IMTP model, specifically tailored to IMTP packing materials, was used for the mass transfer and the interfacial area calculation [46]. Both the absorption and stripping columns were divided into 20 calculation stages. Columns diameters have been determined to avoid flooding for each case and the columns heights have been set to 20m for all the cases. The CC model specifications are presented in Table 5. A pinch point of 15°C was considered for the internal heat exchanger. An efficiency of 0.8 was used for the pumps. A make-up unit was added to the model to ensure a constant flow rate of solvent into the system by compensating the solvent losses in the exhaust gas and the CO_2 stream. The condenser temperature at the top of the stripper was set to 30°C. Using a design specification, the reboiler duty was adjusted to reach a carbon capture rate of 90%. After being captured, the CO_2 must be compressed to be injected into the CO_2 pipelines for further utilization and storage. A multi-stage compressor with intercoolers was used for CO_2 compression. The CO_2 stream was compressed up to 30 bar for pipeline transport. This value is based on the recommendation of Fluxys [47], the gas network operator in Belgium. The compression process consisted of 3 stages, including intermediate cooling to 40°C and removal of condensed water. The total pressure ratio was equally distributed between the 3 compressor stages.

TABLE 5: CARBON CAPTURE MODEL SPECIFICATIONS.

Parameter	Value
CO_2 capture rate (%)	90
Absorber 1st stage pressure (bar)	1.013
Stripper condenser pressure (bar)	1.2
Condenser temperature (°C)	30
Solvent cooling temperature (°C)	40
Pinch internal heat exchanger (°C)	15
Pumps efficiency (%)	80
CO_2 compression stages	3
CO_2 compression intercooling (°C)	40
Compressor outlet CO_2 pressure (bar)	30

In this work, the steam required for the reboiler was not directly extracted from CCGT. Indeed, for all the simulations, the impact of steam extraction or penalty of reboiler duty on the CCGT power was estimated based on the approach described by Zhao et al. [48]. This approach is based on the assumption that the steam extraction would be used in the Carnot cycle [48,49]. The equivalent power loss (ΔP_{loss}) was calculated using the following equation [50].

$$\Delta P_{loss} = \theta_{eff}\ \theta_{carnot}.M_{CO_2}.Q_{reboiler} \quad (9)$$

where θ_{eff} is the effective efficiency of power loss in the water/steam cycle due to steam extraction, θ_{carnot} is the Carnot efficiency of the water/steam cycle, M_{CO_2} is the total CO_2 capture rate and $Q_{reboiler}$ is the reboiler heat duty. θ_{eff} can be calculated by Eq. 10.

$$\theta_{eff} = 0.6102 + 0.00165(T_{sat,steam} - 273.15) \quad (10)$$

and θ_{carnot} is calculated as below.

$$\theta_{carnot} = 1 - \frac{T_{cond}}{T_{sat,steam}} \quad (11)$$

In this work, T_{cond} is the temperature of the cold source, and it has been assumed to be 40°C. $T_{sat,\ steam}$ was assumed to be higher than $T_{reboiler}$ by 10°C. A COP (coefficient of performance) of 10 was used to calculate the electrical power according to the cooling load [25]. COP is defined as the ratio between the cooling load and the electrical power consumed for cooling.

3. RESULTS AND DISCUSSION

This section compares the performance of carbon capture simulations in the CCGT power plant using the novel EGC concept (shown in Fig. 3) with respect to the conventional concepts, CCGT and CCGT with EGR. In the EGR and the EGC case, the O_2 molar concentration at the combustor inlet was maintained at 16% to ensure stable combustor operation. Full load operation of CCGT was simulated at fixed TIT, CPR and CCGT power for all three configurations.

3.1. Impact of EGC on CC Plant

The technical specifications of the DCC and CC plant are given in Table 6 for three different cases: CCGT, CCGT+EGR and CCGT+EGR+EGC. For each case, depending on the exhaust gas properties, the required diameter of the DCC, absorber and stripper columns were determined. Moreover, a sensitivity analysis was performed for each case to determine the optimum Liquid-to-Gas ratio (L/G) for minimizing the reboiler duty in the CC unit. EGR ratio is calculated as the ratio of the recirculated exhaust flow (stream 4) to that of the DCC outlet flow (stream 3).

The performance of the CC plant with the three cases is provided in Table 7. Firstly, the conventional EGR method with turbine cooling from compressor bleed air expectedly reduces the CCGT exhaust mass flow by 35.8% (compared to CCGT without EGR) at an EGR ratio of 0.35. The CO_2 concentration in the exhaust is also incremented by 2.77 p.p. (56.7% increase), leading to a reduction in the CC power penalty by 2.5 MW_e. With the further addition of EGC with EGR, all turbine cooling air is substituted by CCGT exhaust gas, and the EGR ratio could be further increased to 0.40 (11.8% increase) while simultaneously maintaining 16% (mol.) O_2 fraction at combustor inlet. This further increase in EGR ratio is allowed because a part of the recirculated exhaust gas is diverted towards the turbine for cooling with EGC (Fig. 3), so the gas turbine inlet flow is able to accommodate more exhaust gas for the same O_2 fraction for the combustor. Because of this increased EGR ratio, the exhaust flow rate with EGC is further reduced by 91.2 kg/s (a 14.4% reduction compared to EGR), which is a reduction of 45% compared to the CCGT case. More importantly, implementing EGC further

TABLE 6: SPECIFICATIONS OF DCC AND CC PLANT.

	CCGT	CCGT+EGR	CCGT+EGR+EGC
DCC Parameter			
DCC diameter (m)	20.5	20.5	19.8
DCC height (m)	10.0	10.0	10.0
L/G (kg/kg)	1.43	1.50	1.52
Water flow rate (kg/s)	1467.2	1533.0	1447.5
DCC outlet water T (°C)	48.0	49.59	50.28
Inlet exhaust gas specific heat (J/kg/K)	1068.2	1075.7	1079.9
Carbon Capture Plant Parameters			
Absorber diameter (m)	21.1	17.9	16.9
Absorber height (m)	20.0	20.0	20.0
Stripper diameter (m)	9.4	9.3	9.2
Stripper height (m)	20.0	20.0	20.0
Capture rate (%)	90.0	90.0	90.0
L/G (kg/kg)	1.4	2.1	2.4
Solvent flow rate (kg/s)	1385.4	1334.9	1306.6
Specific Reboiler Duty (MJ/kgCO_2)	3.77	3.74	3.72

TABLE 7: PERFORMANCE PARAMETERS OF CARBON CAPTURE PLANT.

Parameter	CCGT	CCGT+EGR	CCGT+EGR+EGC
CCGT exhaust mass flow (kg/s)	1026	1022	952.3
Exhaust mass flow in CC plant (kg/s)	989.57	635.64	544.42
EGR ratio	-	0.35	0.40
CCGT exhaust CO_2 (mol.%)	4.88	7.65	8.82
Exhaust gas blowers (MW_e)	10.41	7.12	6.18
CC reboiler duty (MW_{th})	249.40	246.48	241.92
Cooling load in EGR Loop (MW_{th})	144.49	162.02	157.62
Solvent cooler (MW_{th})	34.70	38.74	41.69
Condenser (MW_{th})	78.23	79.38	78.23
CO_2 compression cooling (MW_{th})	19.81	19.76	19.45
Cooling power (MW_e)	27.72	29.9	29.7
CC reboiler temperature (°C)	104.77	104.94	104.95
CC solvent pumps (MW_e)	0.03	0.03	0.03
CO_2 compression (MW_e)	16.47	16.43	16.17
Total electrical power consumption (EGR+CC) (MW_e)	26.91	23.58	22.37
Equivalent reboiler electrical duty (MW_e)	129.9	128.5	126.2
Total CC power penalty (MW_e)	**184.6**	**182.1**	**178.2**

increases the molar CO_2 concentration in the exhaust by 1.17 p.p., which is a significant increment of 15.32% over the EGR method with conventional blade cooling. Also, compared to baseline CCGT, EGC increases CO_2 concentration by 3.94 p.p. (80.7%), which in the case of conventional EGR only increases by 2.7 p.p. (56.7%). Figure 5 graphically shows the exhaust flow reduction and CO_2 enrichment with EGC compared to conventional EGR.

These improvements are also manifested in the performance of power consumption in the CC plant. The CC reboiler duty is reduced by 1.85%, blower power consumption is reduced by 13.2%, and CO_2 compression load is reduced by 1.5% in the CCGT+EGR+EGC configuration. As a result, the overall CC power penalty is reduced by 3.9 MW_e (2.1% reduction). The benefit of lower exhaust mass flow and higher CO_2 concentration with EGC can also be seen in other sources of power consumption in the CC plant in Table 7. The resulting reduction in the size of the direct contact cooler, absorber and stripper columns is also evident in Table 6. Table 8 provides the mass flow, temperature, pressure and molar concentrations of CO_2, H_2O and O_2 for the key flow streams (shown in Fig. 3) for all three configurations. Overall, these results demonstrate the advantage of the proposed concept of EGC in terms of an increase in overall CCGT efficiency, reduction in exhaust flow and CO_2 enrichment in exhaust. These are solid and promising bases for further techno-economic assessments as EGC can potentially enable reductions in OPEX and CAPEX of the carbon capture process.

TABLE 8: FLOW PARAMETERS AND MOLAR CONCENTRATION OF CO_2, H_2O AND O_2 FOR KEY GAS STREAMS. STREAM NUMBERS ARE SHOWN IN FIGURE 3.

		CCGT						CCGT+EGR						CCGT+EGR+EGC					
Gas Stream	Description	m (kg/s)	T (°C)	P (bar)	X_{CO2} (%)	X_{H2O} (%)	X_{O2} (%)	m (kg/s)	T (°C)	P (bar)	X_{CO2} (%)	X_{H2O} (%)	X_{O2} (%)	m (kg/s)	T (°C)	P (bar)	X_{CO2} (%)	X_{H2O} (%)	X_{O2} (%)
1	Compressor inlet	998.9	15.0	1.01	0.0	1.0	20.7	994.1	20.7	1.01	2.6	2.1	16.0	811.8	20.1	1.01	2.7	2.0	16.0
2	CCGT exhaust	1026.0	80.8	1.01	4.6	9.7	10.9	1022.0	79.6	1.01	7.1	10.8	6.3	952.3	76.9	1.01	8.2	11.5	4.3
3	DCC outlet	989.6	30.0	1.00	4.9	4.3	11.6	977.9	30.0	1.00	7.7	4.3	6.7	907.4	30.1	1.00	8.8	4.3	4.7
4	Recirculated gas	-	-	-	-	-	-	342.3	31.4	1.01	7.7	4.3	6.7	362.9	31.5	1.01	8.8	4.3	4.7
5	Exhaust gas for cooling	-	-	-	-	-	-	-	-	-	-	-	-	113.6	31.5	1.01	8.8	4.3	4.7
6	Exhaust gas to CC	989.6	40.3	1.10	4.9	4.3	11.6	635.6	40.1	1.10	7.7	4.3	6.7	544.4	40.2	1.10	8.8	4.3	4.7
7	Treated exhaust gas	974.6	51.8	1.01	0.5	12.1	11.1	617.7	57.1	1.01	0.7	15.7	6.4	525.1	58.7	1.01	0.8	17.0	4.4

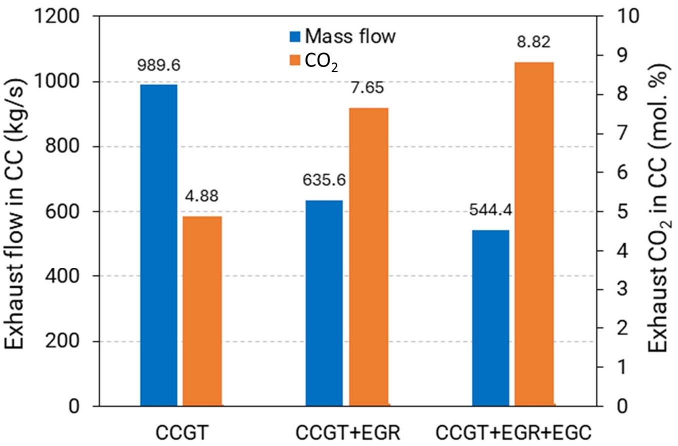

FIGURE 5: REDUCTION IN EXHAUST MASS FLOW AND INCREASE IN EXHAUST CO_2 CONCENTRATION WITH EGC COMPARED TO CONVENTIONAL CCGT WITH EGR AND CCGT WITHOUT EGR.

3.2. Impact of EGC on CCGT performance

Performance parameters of the CCGT power plant with carbon capture are given in Table 9 for the three configurations. The CCGT power and efficiency were calculated without accounting for the carbon capture penalty, while the CCGT net power and efficiency were calculated by subtracting the CC power penalty from the total power. The total penalty from the CC plant was calculated by adding the power consumed in the EGR loop (two blowers and water pump) and the power consumed in all the processes in the CC plant, such as reboiler duty, cooling load, pumps, CO_2 compression, etc. The efficiency was calculated on the fuel LHV basis. Without accounting for the CC penalty, the introduction of EGC increases the CCGT efficiency by about 1.1 p.p. from (63.6% to 64.7%) due to the benefit from the use of exhaust gas with higher specific heat as cooling media instead of air.

Performing carbon capture without any EGR reduces the efficiency from 63.6% to 49.41% (CCGT net efficiency), a significant reduction of over 14 p.p. With conventional EGR, the CC penalty is slightly reduced by around 2.4 MW_e, allowing a slight net efficiency increment of 0.2 p.p. (0.4% increase). With further implementation of EGC, 3.9 MW_e of power is recovered from the CC plant, increasing the net efficiency by 1.15 p.p. to 50.72%. Thus, compared to carbon capture with EGR, which allows only 0.4% recovery in net efficiency (compared to without EGR case), implementing EGC with EGR can increase the power plant efficiency by a much higher value of 2.6%.

TABLE 9: COMPARISON OF CCGT PERFORMANCE WITH CARBON CAPTURE.

Parameter	CCGT	CCGT+ EGR	CCGT+ EGR+EGC
CCGT power (MW_e)	825.3	825.3	825.3
CCGT efficiency (%)	63.6	63.6	64.7
CC power penalty (MW_e)	184.6	182.1	178.2
CCGT net power (MWe)	640.8	643.1	647.1
CCGT net efficiency (%)	49.41	49.57	50.72
Ambient air mass flow (kg/s)	998.9	651.8	562.4
Fuel mass flow (kg/s)	27.2	27.2	26.8
Compressor inlet T (°C)	15	20.7	20.1
CCGT exhaust M (kg/s)	1026	1022	952.3
CCGT exhaust T (°C)	80.8	79.6	76.9
CCGT exhaust P (bar)	1.013	1.013	1.013

This improvement in CCGT and carbon capture performance through EGC is due to the substitution of turbine cooling air with exhaust gas, which, firstly, allows a higher degree of recirculation and, secondly, reduces the required cooling flow due to the higher specific heat of exhaust gas. The cooling flow for all three cooled turbine stages is given in Table 10. As can be seen, the total cooling flow in each turbine stage is significantly lower in the case of EGC, compared to conventional EGR and without EGR case. The marginal increase in the cooling air for the EGR case, compared to no EGR case, is due to a slight increase in cooling air temperature because of the mixture composition change in the compressor with EGR.

TABLE 10: TURBINE COOLING FLOW RATE FOR EACH COOLED STAGE. T1, T2 AND T3 ARE FIRST, SECOND AND THIRD TURBINE STAGE.

	CCGT	CCGT+EGR	CCGT+EGR+EGC
$m_{cl,T1}$ (kg/s)	109.9	110.7	87.9
$m_{cl,T2}$ (kg/s)	46.4	47.4	24.6
$m_{cl,T3}$ (kg/s)	8.7	9.8	1.1
$m_{cl,tot}$ (kg/s)	165	167.9	113.6

The additional power consumed by the EGC compressor (shown in Fig. 3) for pressurizing the exhaust gas from 1 atm to the required entry pressure in each cooled turbine row is shown in Fig. 6. Each row was separately pressurised to the pressure in main gas flow in turbine through different stages in the EGC compressor (shown in Fig. 3). The total power consumed in pressurizing the exhaust gas for all six cooled rows was 11% of the power consumed by the main compressor. More importantly, 64.4 % (30.3 MW_e) of the EGC compression power was consumed by cooling exhaust gas for the first stator itself.

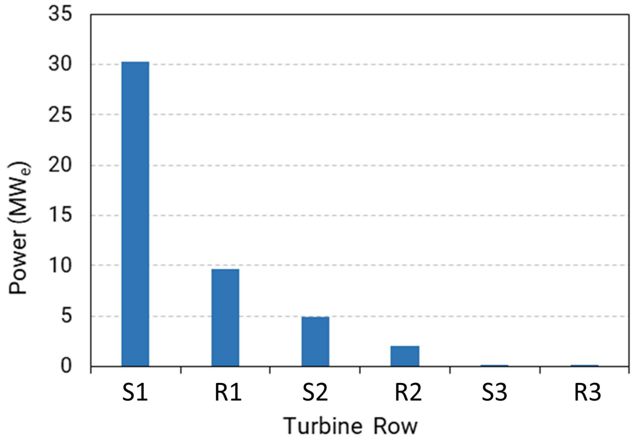

FIGURE 6: POWER CONSUMED IN PRESSURIZING EGC GAS FOR EACH COOLED TURBINE ROW. NUMBER DENOTES THE TURBINE STAGE. S: STATOR; R: ROTOR.

The effect of compressor inlet composition change on the off-design performance of the gas turbine was estimated based on Eq. 12, with the assumption of choked flow at the inlet of the first stator inlet. The stator throat area was estimated for new inlet conditions to see if existing gas turbines can accommodate the change in mass flow due to composition change or not.

$$m = \frac{P}{\sqrt{RT}} A\sqrt{\gamma} M \left(1 + \frac{\gamma - 1}{2} M^2\right)^{\frac{\gamma+1}{2-2\gamma}} \qquad (12)$$

Compared to the CCGT case without EGR, stator throat area change was found to be negligible in the case of EGR and EGC, respectively. This low change shows that the proposed EGC solution can be implemented in existing gas turbines without any hardware modifications. A similar inference was drawn by Li et al. [15] in an early study on EGR with conventional cooling for enhanced carbon capture.

It must be noted that the conventional EGR concept is presently at the theoretical stage, and in fact, the world's first natural gas-fired CCGT with CC using EGR is currently being built and is expected to start operations in 2028 [22]. Most literature studies on EGR are at full load conditions, however, some studies have shown the benefit of EGR on CCGT in terms of plant efficiency and carbon capture process, even at part load conditions [51–54]. This indicates that EGR can meet the requirement of load flexibility in the future electricity market, where power plants will need to operate mostly at part load on a cyclic basis [6]. In this work, the novel concept of EGC was investigated at full load conditions and promising results were obtained in terms of extending the recirculation ratio, reducing exhaust mass flow, enriching exhaust CO_2 and reducing the size of CC plant components. Investigation of the part-load CCGT performance with EGC is part of another ongoing work by authors and will be reported in subsequent publications.

The results discussed in this paper also suggest that EGC can provide considerable benefit to the economics of capturing carbon in CCGT. Unfortunately, adequate data about the capital and operational costs of large CC systems for heavy-duty industrial CCGTs is not available in the open literature [13], which hinders the quantification of the economic benefits from EGC at this stage. Indeed, economic evaluation of conventional EGR is itself limited in literature and some of the available studies have been discussed in section 1.

4. CONCLUSIONS

The study serves as a proof of concept for a novel approach of using exhaust gas recirculation (EGR) for turbine cooling for enhanced carbon capture, referred to as exhaust gas cooling (EGC). A validated latest generation H-class combined cycle gas turbine (CCGT) power plant was modelled with turbine cooling from the recirculated exhaust flow. The CCGT plant was integrated with a carbon capture (CC) unit, and the technical viability of the EGC concept was studied with respect to conventional EGR. The following conclusions can be drawn from the work.

1. Compared to the conventional EGR method, for the same oxygen molar concentration at the combustor inlet (required for stable combustion and low CO emission), implementing EGC can facilitate an increase in EGR ratio from 0.35 to 0.40, leading to a further reduction in the exhaust mass flow by 91.2 kg/s (14.4% reduction over that in conventional EGR) in an H-class CCGT power plant.
2. EGC can also increase the molar CO_2 concentration in the exhaust by 1.17. p.p. (15.32%), compared to conventional EGR, thereby reducing the size of the CC plant components, potentially lower OPEX and CAPEX of the carbon capture process. Compared to conventional EGR, the CC penalty on net electrical power output can also be reduced by 2.1% by using the proposed EGC concept. This reduced CC penalty can improve the power plant's net electrical efficiency by 2.6%, which with EGR could be only improved by 0.4%. As an absolute value, the introduction of EGC increases the CCGT efficiency by 1.1 percentage points (from 49.6% to 50.7%) with respect to CCGT with EGR only. This positive impact from EGC can be divided into its two main contributors: a) benefit from the use of higher specific heat of exhaust gas for cooling, which increases the gross efficiency (without accounting for penalty from carbon capture) of 1.1 percentage points from (63.6% to 64.7%) due to the reduction of cooling mass flow rate and b) the reduction of CC penalty of around 4 MW, that increases the efficiency for the remaining 0.05 percentage points.
3. EGC can be implemented in currently operational machines without major modifications and therefore, it presents an attractive approach for improved carbon capture in practical CCGT power plants.

5. ACKNOWLEDGEMENT

This project has received funding from the European Union's Horizon 2020 research and innovation programme under the Marie Skłodowska-Curie grant agreement No: INSPIRE-956803.

The financial support received from the European Union is gratefully acknowledged.

6. REFERENCES

[1] 2024, *World Energy Outlook 2024*.
[2] 2024, *IEA Electricity 2024: Analysis and Forecast to 2026*.
[3] Olivier, J. G. J., 2022, "Trends in Global CO2 and Total Greenhouse Gas Emissions: 2021 Summary Report," PBL Netherlands Environ. Assess. Agency, **5**(August), pp. 1–11.
[4] Wang, Z., 2016, *Energy and Air Pollution: World Energy Outlook Special Report 2016*.
[5] 2024, "General Electric 9HA.02 Gas Turbine" [Online]. Available: https://www.gevernova.com/gas-power/products/gas-turbines/9ha. [Accessed: 30-Nov-2024].
[6] Gonzalez-salazar, M. A., Kirsten, T., and Prchlik, L., 2018, "Review of the Operational Fl Exibility and Emissions of Gas- and Coal- Fired Power Plants in a Future with Growing Renewables," Renew. Sustain. Energy Rev., **82**(July 2017), pp. 1497–1513.
[7] Ruchti, C., Olia, H., Franitza, K., and Ehrsam, A., 2011, "Combined Cycle Power Plants as Ideal Solution to Balance Grid Fluctuations," *Kraftwerkstechnisches Kolloquium*, TU Dresden, Germany, pp. 18–19.
[8] Orths, A., Anderson, C. L., Brown, T., Mulhern, J., Pudjianto, D., and Ernst, B., 2019, "Flexibility From Energy Systems Integration: Supporting Synergies Among Sectors," IEEE Power Energy Mag., (17(6)), pp. 67–78.
[9] Alqahtani, B. J., and Patiño-Echeverri, D., 2016, "Integrated Solar Combined Cycle Power Plants : Paving the Way for Thermal Solar," Appl. Energy, **169**, pp. 927–936.
[10] 2022, *Global Gas Turbines Market for Power Industry 2023/2027*.
[11] Wilcox, J., 2012, *Carbon Capture*, Springer Science & Business Media.
[12] Gibbins, J., Chalmers, H., Lucquiaud, M., Li, J., Mcglashan, N., Liang, X., and Davison, J., 2011, "Techno-Economic Assessment of CO2 Capture Retrofit to Existing Power Plants," Energy Procedia, **4**, pp. 1835–1842.
[13] Sammak, M., Smith, R., Kulkarni, P., N., R., and Sholes, J., 2024, "Gas Turbine Combined Cycle System Integration with Carbon Capture Plant for Improved Value," *Volume 5: Cycle Innovations*, American Society of Mechanical Engineers, London, England, pp. 1–13.
[14] Mimura, T., Nojo, T., Iijima, M., Yoshiyama, T., and Tanaka, H., 2002, "Recent Developments on Flue Gas CO2 Recovery Technology," *Proceedings of the 6th International Conference on Greenhouse Gas Control Technologies*, Kyoto, Japan, pp. 1057–1061.
[15] Li, H., Haugen, G., Ditaranto, M., Berstad, D., and Jordal, K., 2011, "Impacts of Exhaust Gas Recirculation (EGR) on the Natural Gas Combined Cycle Integrated with Chemical Absorption CO2 Capture Technology," Energy Procedia, **4**, pp. 1411–1418.
[16] Wang, X., and Song, C., 2020, "Carbon Capture From Flue Gas and the Atmosphere : A Perspective."
[17] Gibbins, J., Chalmers, H., Lucquiaud, M., McGlashan, N., Li, J., and Liang, X., 2011, *Retrofitting CO2 Capture to Existing Power Plants*.
[18] Botero, C., Finkenrath, M., Bartlett, M., Chu, R., Choi, G., and Chinn, D., 2009, "Redesign, Optimization, and Economic Evaluation of a Natural Gas Combined Cycle with the Best Integrated Technology CO2 Capture," Energy Procedia, **1**(1), pp. 3835–3842.
[19] Røkke P.E., M., B., A., A., J.P., J., T., M., and K.A., H., 2006, *CO2 Capture at Tjeldbergodden and Transport to Draugen/Heidun*.
[20] ElKady, A. M., Evulet, A., Brand, A., Ursin, T. P., and Lynghjem, A., 2009, "Application of Exhaust Gas Recirculation in a DLN F-Class Combustion System for Postcombustion Carbon Capture," J. Eng. Gas Turbines Power, **131**(3), pp. 1–6.
[21] Ditaranto, M., Hals, J., and Bjørge, T., 2009, "Investigation on the In-Flame NO Reburning in Turbine Exhaust Gas," Proc. Combust. Inst., **32**, pp. 2659–2666.
[22] "Power Engineering" [Online]. Available: https://www.power-eng.com/environmental-emissions/carbon-capture-storage/this-project-aims-to-be-the-first-gas-fired-power-station-with-carbon-capture-and-storage/. [Accessed: 05-Feb-2025].
[23] Biliyok, C., and Yeung, H., 2013, "Evaluation of Natural Gas Combined Cycle Power Plant for Post-Combustion CO2 Capture Integration," Int. J. Greenh. Gas Control, **19**, pp. 396–405.
[24] Nwaoha, C., Odoh, K., Ikpatt, E., Orji, R., and Idem, R., 2017, "Process Simulation, Parametric Sensitivity Analysis and ANFIS Modeling of CO2 Capture from Natural Gas Using Aqueous MDEA-PZ Blend Solution," J. Environ. Chem. Eng., **5**(6), pp. 5588–5598.
[25] Verhaeghe, A., Bricteux, L., Demeyer, F., Blondeau, J., and De Paepe, W., 2024, "Retrofitting an Existing Combined Cycle Gas Turbine With Post-Combustion Carbon Capture: Assessment of Solvent Selection Impact on Performance," *Volume 5: Cycle Innovations*, American Society of Mechanical Engineers, London, England, pp. 1–14.
[26] Mohd Pauzi, M. M., Azmi, N., and Lau, K. K., 2022, "Emerging Solvent Regeneration Technologies for CO2 Capture through Offshore Natural Gas Purification Processes," Sustain., **14**(7).
[27] Baudoux, A., Demeyer, F., and Paepe, W. De, 2024, "Advanced Configurations of Amine Based Post-Combustion Carbon Capture Process Applied to Combined Cycle Gas Turbine," Energy Convers. Manag. X, **22**(February).
[28] Horlock, J. H., Watson, D. T., and Jones, T. V., 2001, "Limitations of Gas Turbine Performance Imposed by Large Turbine Cooling Flows," J. Eng. Gas Turbines Power, **123**(3), pp. 487–494.
[29] Stathopoulos, P., 2018, "Comprehensive Thermodynamic Analysis of the Humphrey Cycle for Gas Turbines with Pressure Gain Combustion," Energies, **11**(12).

[30] Kurzke, J., 2002, "Performance Modeling Methodology: Efficiency Definitions for Cooled Single and Multistage Turbines," Am. Soc. Mech. Eng. Int. Gas Turbine Institute, Turbo Expo IGTI, **1**, pp. 85–92.
[31] Dubey, A., Sorce, A., and Stathopoulos, P., 2024, "A Comprehensive Thermodynamic Analysis of Gas Turbine Combined Cycles With Pressure Gain Combustion Based on Humphrey Cycle," J. Eng. Gas Turbines Power, **147**(February), pp. 1–39.
[32] Wilcock, R. C., Young, J. B., and Horlock, J. H., 2005, "The Effect of Turbine Blade Cooling on the Cycle Efficiency of Gas Turbine Power Cycles," J. Eng. Gas Turbines Power, **127**(1), pp. 109–120.
[33] Traverso, A., Massardo, A. F., Cazzola, W., and Lagorio, G., 2004, "Widget-Temp: A Novel Web-Based Approach For Thermoeconomic Analysis And Optimization Of Conventional And Innovative Cycles," *Proceedings of ASME Turbo Expo 2004*, Vienna, Austria.
[34] Ghigliazza, F., Traverso, A., and Massardo, A. F., 2009, "Thermoeconomic Impact on Combined Cycle Performance of Advanced Blade Cooling Systems," Appl. Energy, **86**(10), pp. 2130–2140.
[35] 2024, "Turbomachinery International: Handbook 2024," **64**(6).
[36] Gülen, S., 2019, *Gas Turbine Combined Cycle Power Plants*, CRC Press, Boca Raton.
[37] Chiesa, P., and Macchi, E., 2004, "A Thermodynamic Analysis of Different Options to Break 60% Electric Efficiency in Combined Cycle Power Plants," J. Eng. Gas Turbines Power, **126**(4), pp. 770–785.
[38] Giuffrida, A., Chiesa, P., and Sordillo, A. P., 2024, "A Thermodynamic Study of Pressure Gain Combustion in Combined Cycles," *79th Annual ATI Congress*, Genova, Italy.
[39] Morimoto, K., Matsumura, Y., Suzuki, K., Wakazono, S., Katoka, M., and Yuri, M., 2021, "Operation Status of 1650 ° C Class M501JAC Gas Turbine at T-Point 2 Power Plant Demonstration Facility," Mitsubishi Heavy Ind. Tech. Rev., **58**(3), pp. 1–10.
[40] Ito, E., Okada, I., Tsukagoshi, K., Muyama, A., and Masada, J., 2010, "Development of Key Technologies for the Next Generation Gas Turbine," *ASME Turbo Expo 2010: Power for Land, Sea, and Air*, Glasgow, UK, pp. 847–860.
[41] "Aspen Plus V14" [Online]. Available: https://www.aspentech.com/en/products/engineering/aspen-plus. [Accessed: 06-Feb-2025].
[42] Verhaeghe, A., Dubois, L., Bricteux, L., Thomas, D., Blondeau, J., and De Paepe, W., 2023, "Carbon Capture Performance Assessment Applied to Combined Cycle Gas Turbine Under Part-Load Operation," J. Eng. Gas Turbines Power, **145**(4), pp. 1–8.
[43] Chen, C. -C, and Evans, L. B., 1986, "A Local Composition Model for the Excess Gibbs Energy of Aqueous Electrolyte Systems," AIChE J., **32**(3), pp. 444–454.
[44] Zhang, Y., Que, H., and Chen, C. C., 2011, "Thermodynamic Modeling for CO2 Absorption in Aqueous MEA Solution with Electrolyte NRTL Model," Fluid Phase Equilib., **311**(1), pp. 67–75.
[45] Zhang, Y., and Chen, C. C., 2013, "Modeling CO2 Absorption and Desorption by Aqueous Monoethanolamine Solution with Aspen Rate-Based Model," Energy Procedia, **37**, pp. 1584–1596.
[46] Giorgetti, S., De Paepe, W., Bricteux, L., Parente, A., and Contino, F., 2017, "Carbon Capture on a Micro Gas Turbine: Assessment of the Performance," Energy Procedia, **105**, pp. 4046–4052.
[47] Fluxys Belgium SA, 2022, "CO_2: Preparing for Network Construction" [Online]. Available: https://www.fluxys.com/fr/projects/ carbon-preparing-to-build-the-network.
[48] Zhao, B., Liu, F., Cui, Z., Liu, C., Yue, H., Tang, S., Liu, Y., Lu, H., and Liang, B., 2017, "Enhancing the Energetic Efficiency of MDEA/PZ-Based CO2 Capture Technology for a 650 MW Power Plant: Process Improvement," Appl. Energy, **185**, pp. 362–375.
[49] Goto, K., Yogo, K., and Higashii, T., 2013, "A Review of Efficiency Penalty in a Coal-Fired Power Plant with Post-Combustion CO2 Capture," Appl. Energy, **111**, pp. 710–720.
[50] Oexmann, J., Hensel, C., and Kather, A., 2008, "Post-Combustion CO2-Capture from Coal-Fired Power Plants: Preliminary Evaluation of an Integrated Chemical Absorption Process with Piperazine-Promoted Potassium Carbonate," Int. J. Greenh. Gas Control, **2**(4), pp. 539–552.
[51] Jonshagen, K., "Exhaust Gas Recirculation to Improve Part Load Performance on Combined Cycle Power Plants," *ASME Turbo Expo 2016: Turbomachinery Technical Conference and Exposition*, ASME, Seoul, South Korea.
[52] Qureshi, Y., Ali, U., and Sher, F., 2021, "Part Load Operation of Natural Gas Fired Power Plant with CO 2 Capture System for Selective Exhaust Gas Recirculation," Appl. Therm. Eng., **190**(May 2021).
[53] Ali, M., Genrup, M., and Nord, L. O., 2024, "Part-Load Thermal Efficiency Enhancement in Gas Turbine Combined Cycles by Exhaust Gas Recirculation," Appl. Therm. Eng., **244**(May 2024).
[54] Alcaráz-Calderon, A. M., González-Díaz, M. O., Mendez, Á., González-Santaló J. M., and González-Díaz, A., 2019, "Natural Gas Combined Cycle with Exhaust Gas Recirculation and CO2 Capture at Part-Load Operation s Alcar A," J. Energy Inst., **92**, pp. 370–381.